




Research Article



Numerical Simulation of Vortex-induced Vibration in Pipes with Different Overhang Heights

Kaijie Zheng, Lin Wang* *School of Mechatronic Engineering, Southwest Petroleum University, Chengdu, 610500, China*

Keywords

Gap ratio,
Vortex-induced vibration,
Near wall,
Vibration characteristics.

Abstract

Resonance due to vortex-induced vibration is the leading cause of fatigue damage in submarine-suspended span pipelines working in harsh environments. The vortex-induced vibration of the pipeline at different overhang heights is investigated using a two-dimensional slicing method, and fourth-order Runge-Kutta solves the pipeline vibration equations. The calculated results show that the root means the square value of the lift coefficient and the mean value of the drag coefficient decrease with the increase of the gap ratio, and gradually stabilize when the gap ratio is greater than 1.2. When the gap ratio is less than 1, the lift force at the upper and lower ends of the pipe is not equal, and the time horizon of the lift and drag coefficients is disordered, with peaks of different amplitudes; the dominant frequency of the pipe vibration is the first-order natural frequency, but the influence of the near-wall surface, the vortex on both sides of the pipe is not completely discharged, resulting in multi-frequency vibration in the downstream direction of the pipe.

1. Introduction

In marine engineering, sea tubes are generally buried beneath the seabed. However, waves and currents cause sediment movement at the bottom of subsea structures and the seabed in their vicinity, a phenomenon we usually refer to as subsea scouring. As the soil is gradually lost to the scouring, the pipeline is exposed to waves and currents, even causing lengths of overhanging sections. As the current passes through the pipeline, it produces alternating shedding vortices at the top and bottom of the pipeline, creating a periodically varying lift resistance in the cross-flow and down-flow directions. When the vortex shedding frequency is close to the inherent frequency of the pipe, resonance occurs, resulting in fatigue damage [1-5]. Therefore, it is essential to study the vortex vibration characteristics of

pipelines at different suspension heights to ensure the safe operation of subsea pipelines.

Overhanging pipes are affected by the near-wall surface, which has a very different form of vortex shedding than a single cylinder, resulting in an inconsistent vortex excitation vibration response [6]. As early as 1981, Tsahalidis and Jones [7] conducted an experimental study of vortex vibration in near-wall pipes and found that the velocity required for vortex vibration in near-wall pipes was greater than the velocity without the presence of a boundary. When the gap ratio is relatively small, the pipe vibration response will be suppressed due to incomplete vortex shedding [8-11]. When the gap ratio is reduced to 0.1, vortex shedding can be completely suppressed by the near wall. When the clearance ratio is greater than 5, the near-wall surface has almost no effect on the cylindrical vibration frequency response; and the near wall surface has a significant effect on power

* Corresponding Author: Lin Wang

E-mail address: lincw_wang@qq.com, ORCID: <https://orcid.org/0000-0003-3660-5178>

Received: 2 February 2023; Revised: 20 February 2023; Accepted: 22 February 2023

<https://doi.org/10.52547/crpase.9.1.2837>

Academic Editor: **He Li**

Please cite this article as: K. Zheng, L. Wang, Numerical Simulation of Vortex-induced Vibration in Pipes with Different Overhang Heights, Computational Research Progress in Applied Science & Engineering, CRPASE: Transactions of Mechanical Engineering 9 (2022) 1–7, Article ID: 2837.

transfer, which will lead to a larger lift coefficient for the same phase velocity than for the isolated cylinder [12-16]. The near-wall surface also affects the vortex shedding on both sides of the cylinder, when the gap is small, the vortex shedding on the top and bottom side of the cylinder is not symmetrical, and the stability of eddy current shedding increases with increasing gap ratio [17-20].

There are more studies on high Reynolds number near-wall cylindrical bypass flow, and fewer studies on vortex vibration, which need further summarized studies on the vortex vibration characteristics of different working conditions. In this paper, we adopt the method of computational fluid dynamics to solve the vibration equation of the pipeline by using the Runge-Kutta method, and carry out a numerical simulation of two-dimensional winding of the submarine-suspended pipeline under high Reynolds number with actual size pipe diameter, and study the effect of the gap ratio on the vortex-induced vibration response of the channel and the law of vortex shedding.

2. Numerical Methods

2.1. Control Equations

Assuming that the fluid in the fluid domain is an incompressible viscous fluid, the RANS equation is chosen as the controlling equation, where the continuity equation is (Eq. (1)):

$$\frac{\partial \bar{u}_i}{\partial x_i} = 0 \quad (1)$$

The momentum equation as Eq. (2)

$$\frac{\partial}{\partial t}(\rho \bar{u}_i) + \frac{\partial}{\partial x_j}(\rho \bar{u}_i \bar{u}_j) = -\frac{\partial \bar{p}}{\partial x_i} + \frac{\partial}{\partial x_j} \left(\nu \frac{\partial u_i}{\partial x_i} - \rho \tau_{ij} \right) + S_i \quad (2)$$

where u_i and u_j denote instantaneous velocities in the x and y directions, respectively; x_i and x_j are Cartesian coordinates in the x and y directions, respectively; t is time; p is pressure; ρ is fluid density; ν is kinematic viscosity, $\nu = \frac{1}{Re}$, where Re is Reynolds number; the Reynolds stress is $\tau_{ij} = -\bar{u}_i' \bar{u}_j'$; the mean strain tensor is $S_i = \frac{1}{2} \left(\frac{\partial \bar{u}_i}{\partial x_j} + \frac{\partial \bar{u}_j}{\partial x_i} \right)$.

The control equations are discretized based on the finite volume method and solved in conjunction with the SST k- ω model in the turbulence model. The coupling of pressure and velocity is performed using the SIMPLE algorithm in both time and space in second-order windward format and the diffusion term in second-order central difference format. The three-dimensional pipe vibration model is simplified to two dimensions using a slicing method to facilitate the study. To fit the actual working conditions, the cylindrical vibration model is simplified to a two-degree-of-freedom mass-spring-damped system, in this paper with the following expressions (Eq. (3)):

$$\ddot{x}(t) + 2\xi\omega_n\dot{x}(t) + \omega_n^2x(t) = \frac{\rho U^2 C_D D}{2m} \quad (3)$$

$$\ddot{y}(t) + 2\xi\omega_n\dot{y}(t) + \omega_n^2y(t) = \frac{\rho U^2 C_L D}{2m} \quad (4)$$

where $\xi = \frac{c}{2\sqrt{km}}$ is the damping ratio of the system, and $\omega_n = \sqrt{\frac{k}{m}}$ is the system intrinsic circular frequency, where k is the system stiffness, and m is the mass per unit length of the column; x , \dot{x} , \ddot{x} represent the displacement, velocity and acceleration of the column in the IL direction respectively; y , \dot{y} , \ddot{y} represent the displacement, velocity and acceleration of the column in the CF direction respectively.

Compared with the Euler method (first-order accuracy) and the modified Euler method (second-order accuracy), the Runge-Kutta method has the advantage of high accuracy and low error, so the fourth-order Runge-Kutta method is used to solve the vibration Eq. (3) and Eq. (4) in the IL and cross-stream directions of the cylinder.

$$k_1 = \frac{F_D}{m} - 2\xi\omega_n\dot{x}(t_n) - \omega_n^2x(t_n) \quad (5)$$

$$k_2 = \frac{F_D}{m} - 2\xi\omega_n \left[\dot{x}(t_n) + \frac{k_1\Delta t}{2} \right] - \omega_n^2 \left[x(t_n) + \frac{\dot{x}(t_n)\Delta t}{2} \right] \quad (6)$$

$$k_3 = \frac{F_D}{m} - 2\xi\omega_n \left[\dot{x}(t_n) + \frac{k_1\Delta t}{2} \right] - \omega_n^2 \left[x(t_n) + \frac{\dot{x}(t_n)\Delta t}{2} + \frac{k_1\Delta t^2}{4} \right] \quad (7)$$

$$k_4 = \frac{F_D}{m} - 2\xi\omega_n [\dot{x}(t_n) + k_3\Delta t] - \omega_n^2 \left[x(t_n) + \dot{x}(t_n)\Delta t + \frac{k_2\Delta t^2}{2} \right] \quad (8)$$

$$x(t_{n+1}) = x(t_n) + \dot{x}(t_n)\Delta t + \frac{1}{6}\Delta t(k_1 + 2k_2 + 2k_3 + k_4) \quad (9)$$

where Δt is the time step.

In order to solve the equation, we need to set the initial conditions for the equation. Before the cylinder starts to move, we can get the values of the coordinates of the center point of the cylinder $x(0)$ and $y(0)$ from the model dimensions, and $\dot{x}(0)$ and $\dot{y}(0)$ from the initial velocity set.

2.2. Model Building

This time, a two-dimensional slicing model is used to investigate the effect of different clearance ratios on the vortex vibration of the pipe. The dimensions of the calculation domain are shown in Figure 1. The cylinder diameter is adopted from the actual subsea pipeline dimensions $D = 219mm$. The distance between the center of the cylinder and the velocity inlet and the upper wall is $10D$, the distance from the pressure outlet is $30D$, the distance from the lower wall is set to e , and the clearance ratio $H = e/D$. The first two-order Natural frequencies are $0.53Hz$ and $1.49Hz$ respectively. To ensure the maximum amplitude, the damping ratio is set to 0, and the pipe mass ratio is 6.16.

The model was discretized using a structured mesh, and the area near the column was encrypted, and the boundary

layer mesh height was set so that the dimensions satisfied y^+ equal to 1. For space reasons, only the meshing diagram for $e=0.2$ is shown in Figure 2.

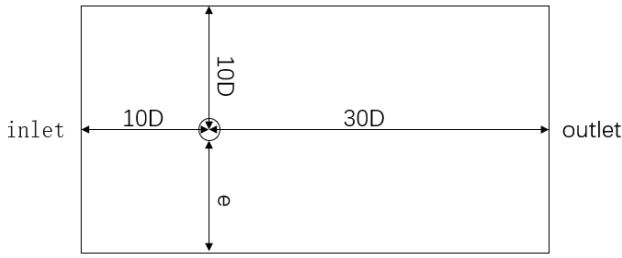


Figure 1. Calculation domain

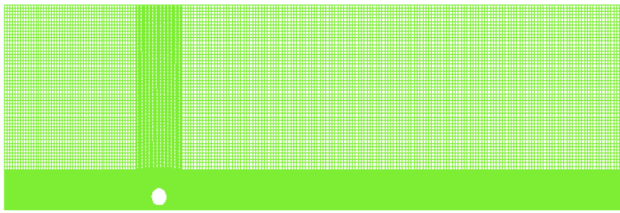


Figure 2. Grid division

2.3. Model Validation

The mesh-independence was verified by taking a working condition with $Re = 1000$. As can be seen from Table 1, the difference in steady-state drag coefficient C_D between Mesh2 and Mesh1 is 18.3%, and the difference in calculated results compared to Mesh3 is 2.7%. It can be seen that Mesh2 already meets the calculation accuracy requirements, so Mesh2 is chosen as the calculation model in this paper. Time step Δt is set to 0.005s, which satisfies $C_o = \frac{U\Delta t}{\Delta x} \leq 1$.

Table 1. Grid irrelevance validation table ($Re=1000$)

Mesh	Elements	C_D
Mesh1	45675	0.89
Mesh2	65870	1.09
Mesh3	83620	1.06

In order to verify the accuracy of the numerical method used in this paper, the working condition with a clearance ratio of 10D was chosen, and the calculation was carried out by taking different points in the Reynolds number Re range from 100 to 300000 to verify the steady state drag coefficient of cylindrical winding. The results are shown in Figure 3. It can be seen that the simulation results in this paper differ from the values from the Hoerner test, the errors are small and acceptable, indicating that the calculation results are reliable.

3. Analysis of Calculation Results

This time, the sea conditions near platform No. 2 in the center of Bohai Bay of Shengli Oilfield were used as a reference, and the specific sea current velocities are shown in Table 2.

The pipeline is generally buried at a depth of 1.5m from the top of the natural mud surface, so the seawater flow velocity at the pipeline can be referred to as the bottom flow velocity. The density of seawater is 1025 kg/m^3 , and the

kinematic viscosity of seawater is $1.05 \times 10^{-6} \text{ m}^2/\text{s}$. The pipeline's diameter is 219 mm as a reference, and the Reynolds number range is 185993~281571 according to the one-year flow rate and the 50-year flow rate.

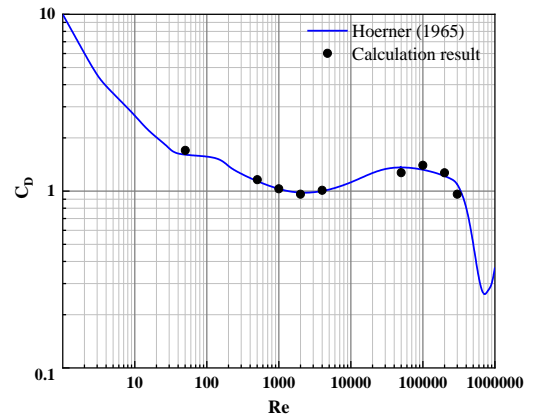


Figure 3. Verification of steady-state drag coefficient

Table 2. Bohai Sea Current Velocity

	Flow rate (m/s)		
	Surface layer	Middle Level	Ground floor
1 year 1 encounter	1.02	0.91	0.87
Once in 50 years	1.71	1.55	1.35

3.1. Fluid Force Coefficient Characteristics

Figure 4 shows the time domain plot of the lift drag coefficient for the clearance ratio 0.2 to 2 operating conditions. As can be seen from Figure (a) and (b), although the drag coefficient still shows a cyclical fluctuation pattern in the 0.2 to 2 clearance ratio range, the time domain waveform peaks of the drag coefficient are not the same in adjacent cycles, and there are significantly high and low peaks, showing a multi-frequency phenomenon. As the gap ratio decreases, the more violent the fluctuation of the drag coefficient is, the more turbulent the waveform becomes. At the same time, the values of the adjacent cycles of the lift coefficient are not equal, and the mean value of the lift coefficient is much larger than zero when the gap ratio is less than 0.6. The smaller the gap ratio, the larger the mean value. In addition, the lift coefficient increases as the gap ratio decreases due to the influence of the vortex shedding at the lower end of the pipe near the wall.

In order to observe more intuitively the law between the lift and drag coefficients and the clearance ratio, the root means square and mean values of the lift and drag coefficients were processed, respectively. The processing results are shown in Figure 5. It can be found that the average drag coefficient and the root mean square value of the lift coefficient decrease with the increase of the clearance ratio. The decrease ratio from the maximum value to the minimum value is 42% and 77%, respectively. Thus, the influence of the clearance ratio on the lift coefficient is much larger than the drag coefficient. When the clearance ratio is more significant than 1.2, its influence on the lift drag coefficient gradually becomes smaller, and the average drag coefficient and the root mean square value of the lift coefficient gradually tend to stabilize. From the slope of the curve, change can be seen. The smaller the clearance ratio on the

lift resistance coefficient, the more significant it can be seen that the vortex drainage influences wall surface is massive.

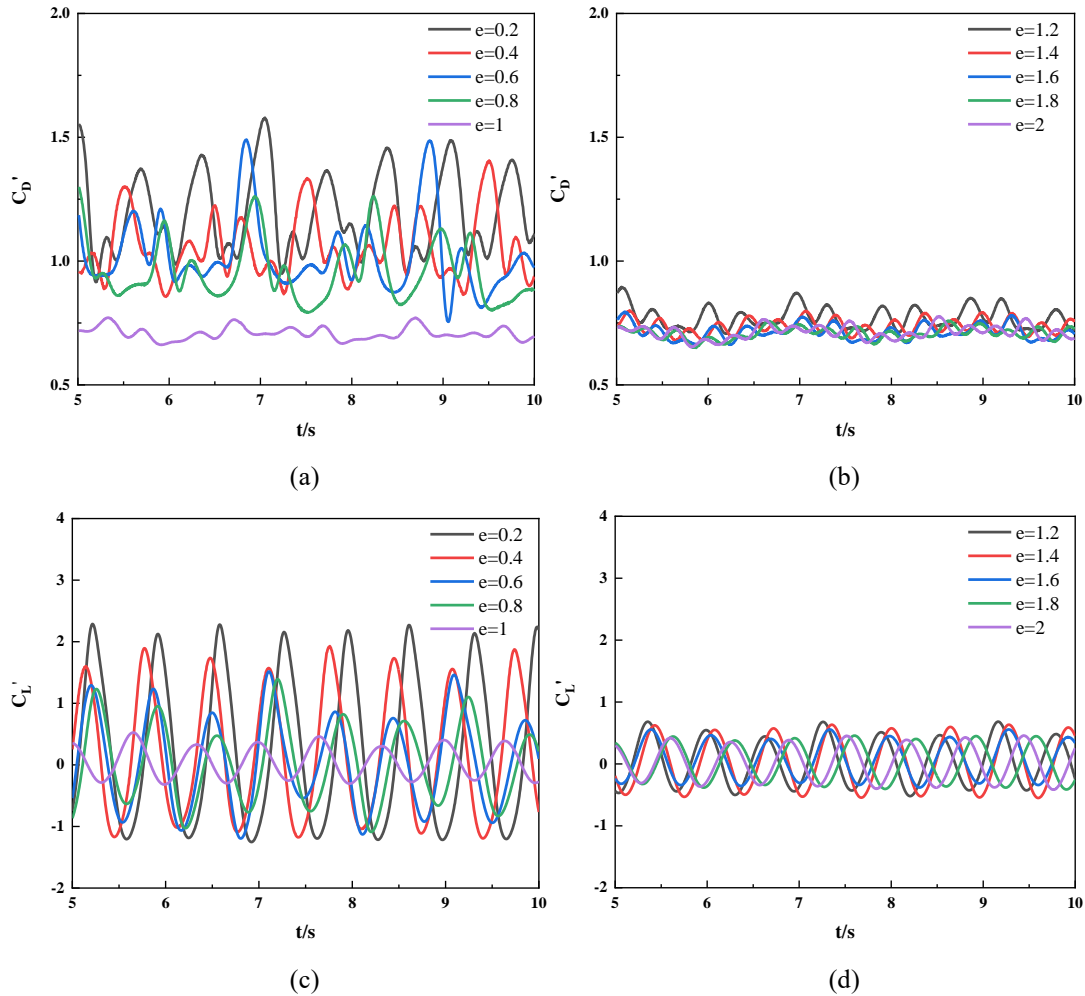


Figure 4. Time domain diagram of transient lift and drag coefficients (where a and b are drag coefficients and c and d are lift coefficients)

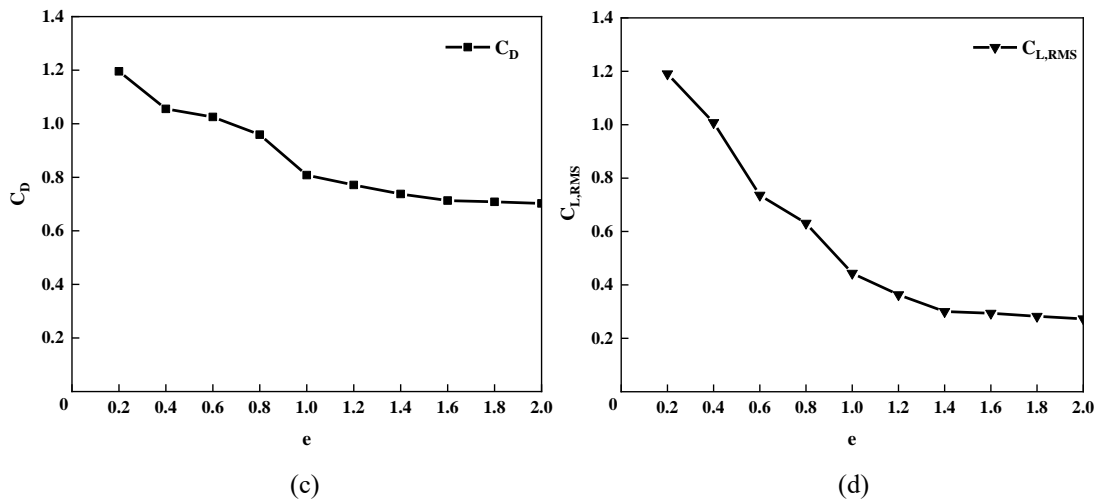


Figure 5. Lift drag coefficient (where a is the mean drag coefficient and b is the root mean square of the lift coefficient)

3.2. Tail Flow Characteristics

The velocity clouds for different gap ratios are shown in Figure 6. The velocity cloud diagram for the gap ratio greater than 1.2 shows that there are two separate vortex shedding at the upper and lower ends of the pipe alternately, and the vortex shedding is shown as 2S mode. When the gap ratio is small, the flow velocity at the lower end of the pipe is more

significant than that at the upper end. The unequal flow velocity at the upper and lower ends of the pipe leads to unequal pressure difference values on both sides, which is the reason why the mean value of the lift coefficient is not zero. When the gap ratio is less than 1, the vortex release by the near wall surface is more influenced. At this time, the

lower end of the vortex can not form a complete release process, showing an irregular shape, and the first half of the tail flow of the vortex's upper and lower side size is inconsistent. At the same time, the dark blue area at the front of the pipe with zero velocity tends to decrease as the gap ratio decreases. This is because when the gap ratio is small, the boundary layer at the lower end of the pipe is influenced by the superficial flow velocity. When the pipe moves

downwards, the water at the lower end is squeezed to move upwards towards the front of the pipe, resulting in a higher velocity at the front end. At clearance ratios of 0.6 and 0.8, it can be observed that the lower-end vortex moves upwards under the action of the water flow and the wall, interacting with the upper-end vortex and merging. When the clearance ratio is more significant than 1.2, the vortex is less affected by the wall and can be discharged typically.

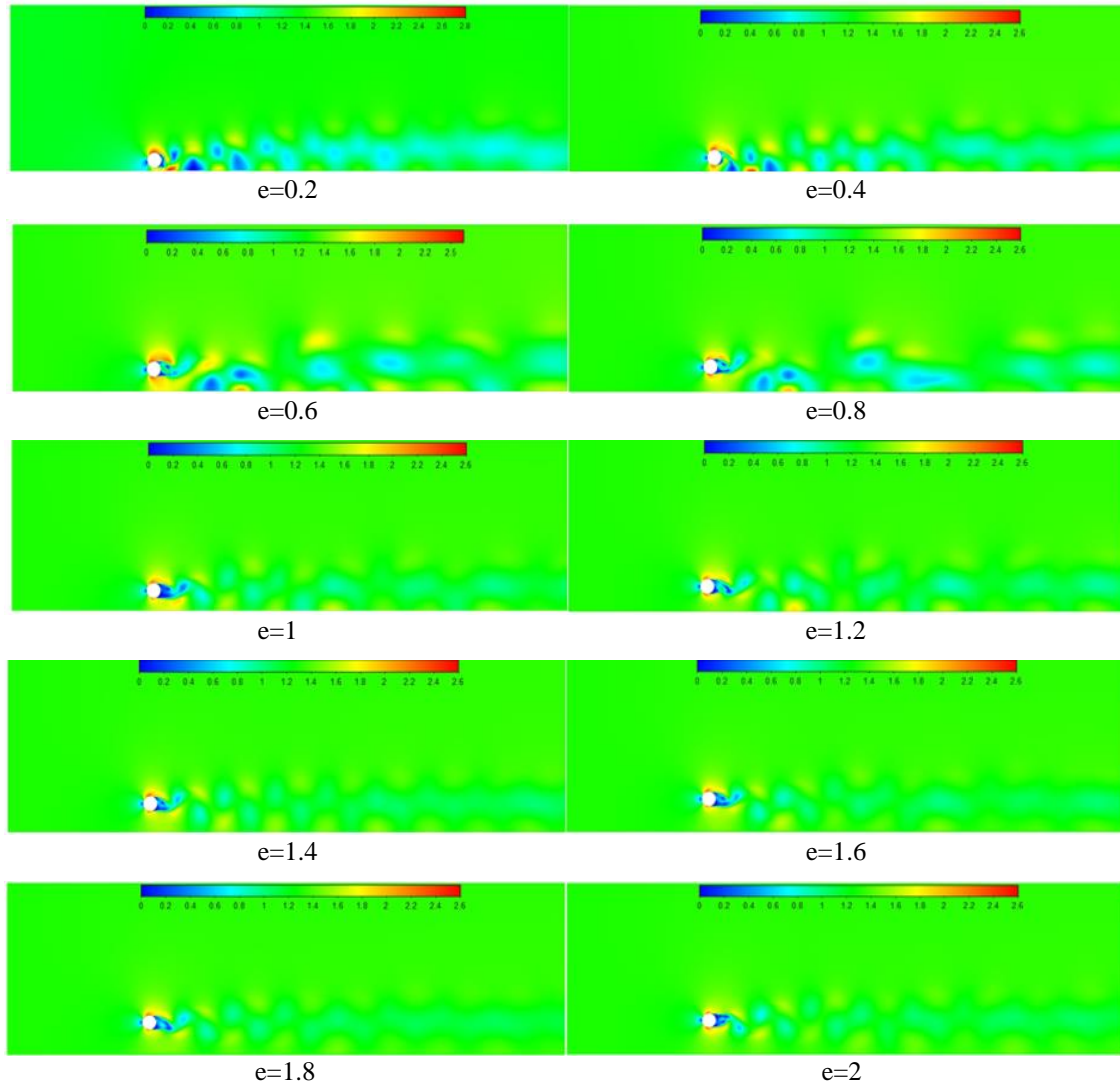


Figure 6. Velocity clouds with different clearance ratios

3.3. Magnitude and Frequency Characteristics

The vibration displacement amplitude and frequency curves for the pipe are shown in Figure 7. A and b are the displacement amplitude-frequency curves in the IL direction, and c and d are the displacement amplitude-frequency curves in the cross-flow direction. It can be found that the dominant frequency of the cross-flow and down-flow vibration of the riser is mainly 0.56Hz, which is close to the first-order intrinsic frequency of the pipe of 0.53Hz, in addition to a small peak close to the second-order intrinsic frequency. It can be found that when the gap is small, there is no significant effect on the vibration frequency in the cross-flow direction of the pipe, although the wall surface will change the vortex-shedding pattern. For pipe down-flow vibration, when the gap ratio is less than 0.8, there is a small peak near

the primary vibration frequency, showing a multi-frequency vibration phenomenon, which does not occur when the gap ratio is greater than or equal to 1. The IL vibration of the pipe is related to the resistance, which is caused by the shedding of each pair of vortices. It can be seen that when the gap ratio is small, the water at the lower end of the pipe will roll upwards during the movement of the pipe, affecting the shedding of the vortices in the tail vortex area. The two vortices in each pair interfere with each other as they move in front of the pipe, resulting in the generation of differential pressure resistance that is not uniform, leading to the existence of multi-frequency vibrations in the IL vibration. However, the reduction in the gap ratio does not affect the frequency of vortex shedding from the pipe, as evidenced by

the cross-flow pipe vibration not exhibiting multi-frequency vibrations.

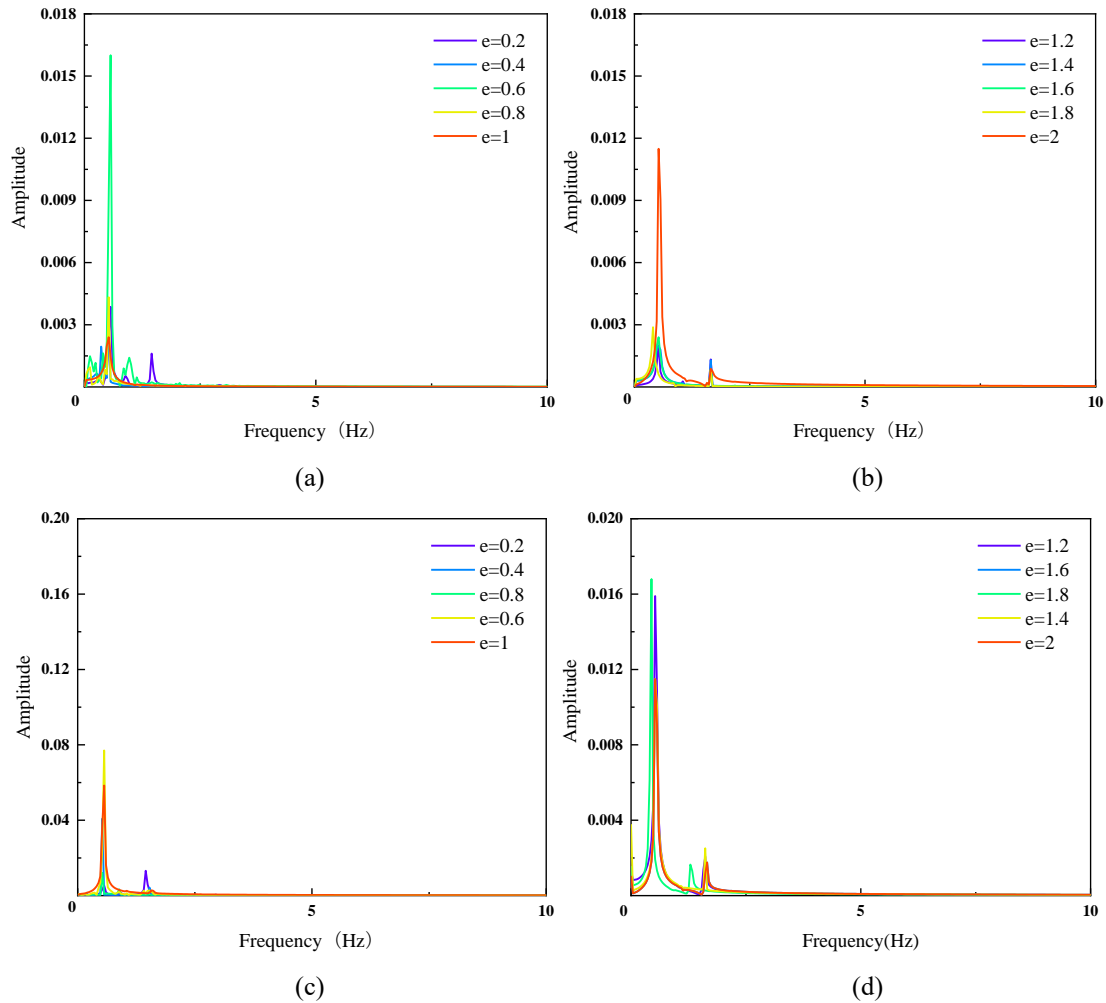


Figure 7. Amplitude and frequency curves of pipe vibration displacement for different clearance ratios (a and b are in the IL direction, c and d are in the CF direction)

4. Conclusions

Based on the mean Reynolds number method and the SST $k-\omega$ turbulence model, two-dimensional numerical simulations of vortex-induced vibration in pipes with different clearance ratios were carried out, mainly to analyze the effects of different clearance ratios on the flow force coefficient characteristics, wake characteristics, and the amplitude and frequency characteristics of pipe vibration.

The root means the fair value of the lift coefficient, and the root means the fair value of the drag coefficient of the subsea suspended pipe decrease as the gap ratio increases. The peak values of the lift and drag coefficients are not the same in adjacent cycles when the gap ratio is small, and the magnitude of the lift force is not the same on both sides of the pipe.

When the gap is relatively small, by the influence of the near wall, the vortex is not complete release; when the gap ratio is more significant than 1.2, the vortex off by the wall influence is gradually reduced.

When the gap is relatively small, small peaks will appear near the center frequency of the pipe vibration in the downstream direction, and the phenomenon of multi-frequency vibration will not occur in the cross-flow direction.

References

- [1] M.P. Paidoussis, A review of flow-induced vibrations in reactors and reactor components, *Nuclear Engineering and Design*. 74 (1983).
- [2] C.H.K. Williamson, Vortex dynamics in the cylinder wake, *Annu Rev Fluid Mech*. 28 (1996).
- [3] N. Jauvtis, C.H.K. Williamson, The effect of two degrees of freedom on vortex-induced vibration at low mass and damping, *J Fluid Mech*. 509 (2004) 23–62.
- [4] B.M. Sumer, J. Fredsøe, *Hydrodynamics around cylindrical structures* (revised edition), 2006.
- [5] J. Guo, Y.F. Li, W. Peng, H.Z. Huang, Bayesian information fusion method for reliability analysis with failure-time data and degradation data, *Qual Reliab Eng Int*. 38 (2022).
- [6] P.W. Bearman, M.M. Zdravkovich, Flow around a circular cylinder near a plane boundary, *J Fluid Mech*. 89 (1978).
- [7] D.T. Tsahalis, W.T. Jones, Vortex-induced vibrations of a flexible cylinder near a plane boundary in steady flow, in: *Proceedings of the Annual Offshore Technology Conference*, 1981.
- [8] M. Yazdi, A Short Communication: An Economic Assessment of Offshore Natural Gas Transferring Pipeline. *Computational Research Progress in Applied Science & Engineering* 7 (2021) 1-4.
- [9] S. Sarkar, S. Sarkar, Vortex dynamics of a cylinder wake in proximity to a wall, *J Fluids Struct*. 26 (2010).

- [10] V. Jacobsen, M.B. Bryndum, R. Nielsen, S. Fines, Cross-flow vibrations of a pipe close to a rigid boundary, *Journal of Energy Resources Technology, Transactions of the ASME*. 106 (1984).
- [11] X.K. Wang, Z. Hao, S.K. Tan, Vortex-induced vibrations of a neutrally buoyant circular cylinder near a plane wall, *J Fluids Struct.* 39 (2013) 188–204.
- [12] M.J. Chern, G.T. Lu, Y.H. Kuan, S. Chakraborty, G. Nugroho, C.B. Liao, T.L. Horng, Numerical Study of Vortex-Induced Vibration of Circular Cylinder Adjacent to Plane Boundary Using Direct-Forcing Immersed Boundary Method, *Journal of Mechanics*. 34 (2018).
- [13] S. Fu, Y. Xu, Y. Chen, Seabed Effects on the Hydrodynamics of a Circular Cylinder Undergoing Vortex-Induced Vibration at High Reynolds Number, *J Waterw Port Coast Ocean Eng.* 140 (2014).
- [14] Z. Huang, C.M. Larsen, Large eddy simulation of an oscillating cylinder close to a wall, in: *Proceedings of the International Conference on Offshore Mechanics and Arctic Engineering - OMAE*, 2010.
- [15] Z. Li, W. Yao, K. Yang, R.K. Jaiman, B.C. Khoo, On the vortex-induced oscillations of a freely vibrating cylinder in the vicinity of a stationary plane wall, *J Fluids Struct.* 65 (2016).
- [16] D.M.Y. Tham, P.S. Gurugubelli, Z. Li, R.K. Jaiman, Freely vibrating circular cylinder in the vicinity of a stationary wall, *J Fluids Struct.* 59 (2015).
- [17] P. Ouro, V. Muhawenimana, C.A.M.E. Wilson, Asymmetric wake of a horizontal cylinder in close proximity to a solid boundary for Reynolds numbers in the subcritical turbulence regime, *Phys Rev Fluids*. 4 (2019).
- [18] M.S. Alasta, A.S. Ali Ali, S. Ebrahimi, M. Masood Ashiq, A. Sami Dheyab, A. AlMasri, A. Alqatanani, and M. Khorram, Modeling of Local Scour Depth Around Bridge Pier Using FLOW 3D. *Computational Research Progress in Applied Science & Engineering* 8 (2022) .
- [19] R. Wang, X. Liu, H. Zhu, D. Zhou, Y. Bao, H. Xu, Dynamics and stability of the wake behind a circular cylinder in the vicinity of a plane moving wall, *Ocean Engineering*. 242 (2021) 110034.
- [20] L. Chen, Y. Dong, Y. Wang, Flow-induced vibration of a near-wall circular cylinder with a small gap ratio at low Reynolds numbers, *J Fluids Struct.* 103 (2021) 103247.